IOP Publishing Plasma Physics and Controlled Fusion
Plasma Phys. Control. Fusion **61** (2019) 085013 (8pp) https://doi.org/10.1088/1361-6587/ab24a4

Electron cyclotron emission based *q*-profile measurement and concept for equilibrium reconstruction

A O Nelson[1], M E Austin[2] and E Kolemen[3]

[1] Princeton Plasma Physics Laboratory, Princeton, NJ 08543, United States of America
[2] University of Texas, Austin, TX 78712, United States of America
[3] Princeton University, Princeton, NJ 08544, United States of America

E-mail: ekolemen@pppl.gov

Received 15 October 2018, revised 30 April 2019
Accepted for publication 24 May 2019
Published 21 June 2019

Abstract

Measuring the plasma equilibrium is essential for real time plasma control and for the investigation of an abundance of physics questions. However, many existing kinetic equilibria reconstruction techniques rely heavily on integrated magnetic measurements and neutron-sensitive diagnostics, which will be difficult to design and operate in ITER and DEMO. Here we present and test a conceptual design for a non-magnetic equilibrium reconstruction method using data from a radial electron cyclotron emission diagnostic and an image of the plasma boundary —diagnostics which can be robustly designed in high-neutron environments. This technique is based on the measurement of a discrete *q*-profile and the symmetry mapping of the electron temperature profile, both of which can be acquired with ECE.

Keywords: equilibrium, *q*-profile, ECE, EFIT, ITER

(Some figures may appear in colour only in the online journal)

1. Introduction

As progress is made towards burning plasmas, intense nuclear environments set stringent demands on the engineering of many diagnostic systems. For example, Thomson scattering (TS) and other optical systems demand both high optical throughput and substantial neutron shielding, requiring the use of mirrors in the optical system [1, 2]. The task of designing optically stable mirrors in a nuclear environment is complicated, and is the subject of ongoing research [3–5]. In contrast, microwave diagnostics such as electron cyclotron emission (ECE) require only waveguides and antennas near the plasma, rendering these techniques robust and well suited to high-neutron environments [1, 6]. As a result, ECE will be a key component of the diagnostics suite on future tokamaks, including ITER [7]. For ITER, two ECE instruments are planned: a multichannel radiometer for profile measurements and a Michelson interferometer for multi-harmonic spectral measurements [8].

ECE provides data that can be used for real time plasma control and physics studies by measuring the electron temperature (T_e) profile, electron temperature fluctuations, power radiated in the electron cyclotron frequency range (70–1000 GHz), and the runaway electron spectrum. In ITER, ECE instruments will cover radial and oblique views in order to diagnose possible distortions in the electron momentum distribution [8]. Importantly, the existence and location of magnetic islands formed by tearing modes can be detected through ECE analysis. Magnetics islands rotate with the plasma and change the temperature profile over a radial region. Since the X-point has a steeper electron temperature gradient than the O-point, a temperature measurement at a fixed toroidal location can detect fluctuations at the frequency of the mode that vary radially and are phase inverted at the center of the island [9]. In addition to tearing modes, it is also possible to detect the existence and spatial structure of Alfvén eigenmodes (AE) with ECE [10, 11].

It is shown in this paper that it is possible to use ECE to detect the location of several such modes simultaneously. The main experimental requirement for this method is that ECE measurements extend across all the modes with sufficient radial density to accurately determine the mode location. In combination with transient magnetics measurements to determine the mode number $q = m/n$ associated with each

island, a q-profile can be constructed out of a discrete set of mode-location pairs. In this paper we describe the algorithm used to determine the radial locations of several coexisting modes from ECE data and demonstrate the technique for a discharge in DIII-D where multiple modes are present.

Most importantly, we also outline a potential technique that could be used to determine a solution of the Grad–Shafranov equation based on ECE measurements without extensive use of integrated magnetic diagnostics. Many existing equilibrium reconstruction methods already use ECE data to improve a magnetics-based Grad–Shafranov solution. T_e has long been used as an internal topographic constraint that can be used to constrain the current profile and magnetic measurements [12, 13]. T_e measurements have also been used to find the magnetic axis in preparation for equilibrium reconstruction [14]. Recently, Qian *et al* demonstrated an iterative solution to the Grad–Shafranov equation using external magnetics and the $m/n = 1/1$ location from ECE [15]. However, all of these approaches require extensive use of integrated magnetic measurements, which will be difficult to implement on ITER and DEMO because of the long discharge duration. In contrast, methods that do not use extensive magnetics have also avoided the use of ECE. Previous non-magnetic equilibrium reconstruction strategies have used polarimetry [16, 17] and motional Stark effect (MSE) [18] to generate a q-profile. In this work, we present the design of a non-magnetic equilibrium reconstruction technique that is based on a radial ECE diagnostic, which is well-suited to high-neutron environments. As is shown below, this method requires access only to the plasma boundary (which is available for example through plasma imaging [19–21]) and the q and T_e profiles, both of which can be taken directly from ECE. The proposed method could be further developed into a stand-alone equilibrium reconstruction tool or be implemented as a value-add to existing reconstruction codes that are based on integrated magnetics.

2. Algorithm

Various methods have been previously developed to determine the location of magnetic islands from radial ECE data. These include the cross correlation of neighboring channels of a multichannel ECE diagnostic [22], direct detection of the island center from the electron temperature perturbation profile [23], temperature oscillation correlation with a Mirnov reference signal [24] and real-time determination of mode location from the matched amplitudes of temperature fluctuations [25]. Further techniques including x-ray imaging spectroscopy [26] and oblique ECE measurements [27, 28] have also been developed to find the radial location of a large tearing mode. All of these methods are derived from the altered radial temperature profile resulting from a rotating magnetic island.

In this work we determine the location of several coexisting modes directly from ECE data via phase-based cross-correlation between adjacent ECE channels on a multichannel ECE radiometer. Dual-phase demodulation using a Mirnov reference signal following the methods in [29] is used to confirm the island locations. The safety factor $q = m/n$ that corresponds to each mode is extracted from instantaneous magnetics using the `modespec` code [30], though q could also be extracted from a full-coverage radial ECE radiometer and an ECE-imaging array. Using the radial position of the mode determined by ECE analysis and $q = m/n$ from `modespec`, the $q(R)$ profile is constructed.

The algorithm used to determine the radial location of a mode is explained below.

1. A time interval of interest is chosen to generate the following discreetly sampled variables:
   - $s = [1, 2, \ldots, N_s]$ = sample number, depends linearly on time,
   - $T_e(i, s)$ = electron temperature at each sample for each ECE channel i,
   - $f_B(j)$ = frequencies of each magnetic mode present in the time interval; ($j = 1, 2, \ldots, N_{\text{modes}}$ where N_{modes} is the number of modes).
2. For each frequency in f_B, a bandpass filter centered on $f_B(j)$ is applied to the ECE data in $T_e(i, s)$. The ECE phase information related to each mode j is then be extracted with a discrete Hilbert transform:
   - $\tilde{T}_e(i, s) = \mathcal{H}[\, T_e(i, s)]$,
   - $\phi(i, s) = \texttt{atan2}[\, \text{Im}(\tilde{T}_e(i, s)), \text{Re}(\tilde{T}_e(i, s))] =$ phase of signal.
3. The phase shift by π between adjacent channels along the radial profile in the presence of a magnetic island is detected via cross-correlation between neighboring ECE channels:
   - $X(i, s) = \sum_k \phi(i - 1, s)\phi(i, s - k)$.

     In-phase channels will have peaks in $X(i, s)$ that are aligned with peaks in the phase signal $\phi(i, s)$, whereas the convolution function $X(i, s)$ between two channels with a phase shift will exhibit a phase shift of π compared to $\phi(i, s)$.
4. The location of the phase shift is mapped to a radial location R using the locations of the ECE channels. A q-profile can then be constructed given a value $q = m/n$ for each mode, which is determined externally.

3. Measurement of the *q*-profile in multi-mode discharges

As a demonstration of the above technique, we use a 40 channel radial ECE radiometer on DIII-D [31] to determine the island locations for a discharge with multiple modes. Figure 1 shows magnetic analysis of DIII-D discharge 163117, where four unique modes ($m/n = 1/1, 5/2, 5/3$ and $6/4$) are present between $t = 4340$ ms and $t = 4390$ ms. Note that resonances of the same mode (such as $2/2$ and $1/1$), though occasionally visible in the Mirnov data, occur at the same $q = m/n$ and thus provide no extra information about the q-profile. Similarly, the artifacts labeled as $m/n = 1/1$ modes between $t = 4340$ ms and $t = 4390$ ms do not correspond to a real mode and do not show up in the ECE spectrum, such that only four distinct modes exist during this time interval. Further, it is noted that this discharge does not

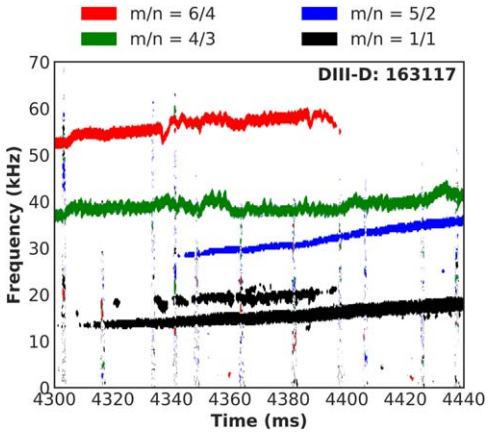

Figure 1. Spectrogram of the Mirnov signal for DIII-D discharge 163117, showing $m/n = 1/1$, $5/2$, $4/3$ and $6/4$ modes at $t = 4361$ ms.

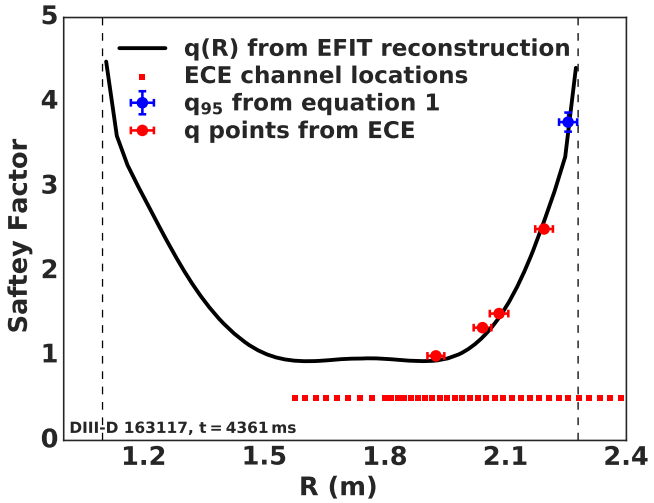

Figure 2. Comparison between (black curve) equilibrium reconstruction from external magnetics and E_R-corrected MSE constraints [32] and (red points) the radial locations of the $m/n = 1/1, 5/2, 4/3$ and $6/4$ modes found with ECE for DIII-D discharge 163117 at $t = 4361$ ms. Four modes can be found within the available ECE coverage. Also shown is an approximation for q_{95} from equation (1) (blue point.)

exhibit Alfvénic MHD activity, which could be used as an additional q-profile constraint as discussed below.

The radial location of all four tearing modes can be found with ECE analysis as described above. The q values from `modespec` are plotted against the radial location from ECE analysis in figure 2. The discrete q-profile obtained here from ECE analysis agrees well with the q-profile extracted from an equilibrium reconstruction on the same discharge that was generated from integrated magnetic and MSE constraints. Note that in the present analysis, the radial location of each ECE channel is determined directly from the vacuum toroidal field. As such, the error bars displayed in figure 2 represent the distances between the adjacent ECE channels. For this discharge the separation of ECE channels is the largest error contributor to q-profile localization; thermal broadening and relativistic shifts are not generally an issue at DIII-D. The effect of the poloidal field B_P is incorporated into the radial measurement error since B_P might not be known during the equilibrium reconstruction process presented in this work. Note that localization of ECE channels on ITER will likely be more difficult due to resolution-limiting effects (discussed below) from higher plasma temperatures.

The techniques described above may also be applied in reverse to determine the poloidal mode number of a magnetic island when a corresponding magnetic analysis fails. This is accomplished by matching the radial location of a resonant surface with an existing q-profile. For example, consider the 17 kHz, $n = 2$ mode present in DIII-D discharge 166578 around $t = 5000$ ms. Magnetic analysis suggests that this mode has $m/n = 5/2$ at 4999 ms and $m/n = 3/2$ at 5001 ms. The discrepancy in these mode numbers is unphysical and results from distorted poloidal magnetic array data, leaving the diagnosis of this mode uncertain. ECE analysis, however, is able to map the mode to the $m/n = 2/2$ surface with high fidelity, thereby determining the poloidal mode number, as shown in figure 3.

In figure 3, the blue curve is a standard dual-phase decomposition algorithm [29] that localizes the tearing mode around the zero crossing of the phase signal as a function of ECE channel number. In discharges with multiple islands, this signal is often distorted far from the mode location by the propagation of other magnetic disturbances in the plasma. In this case, dual-phase decomposition suggests three possible mode locations for discharge 166578. Phase-based cross-correlation between adjacent channels as presented in this paper is shown in figure 3 as black points, and the mode location is manifested by a phase shift of π. Note that the two techniques are plotted on different vertical scales. Phase-based cross-correlation presents only a single mode location in this example, and is found by the authors to yield generally cleaner results when multiple modes exist within a discharge.

This analysis can be used on any discharge where multiple modes can be located with ECE to either verify complete q-profiles generated through other methods or, if enough modes are present, to construct a full q-profile directly from ECE data. It is not necessary, however, to have several co-existing tearing modes in a discharge in order to generate a q-profile with this technique, as discrete q-profile locations can be supplemented with information from other sources. The radial locations of other modes, such as AE, can also be detected with ECE and may provide information on the q-profile [10, 11]. As examples, Nave *et al* have used AE cascades to determine both the value and location of $q_{\min}$ on JET and have used this information to help inform EFIT choice [33] and Kramer *et al* have used TAEs to directly measure the q-profile within the $q = 1$ surface on JT-60U [34, 35]. Additionally, since it possible to excite tearing modes by perturbing the plasma with counter ECCD or 3D magnetic perturbations [36–38], there are a wide variety of tokamak discharges where the measurement of one to a few q values with ECE is possible, even if no tearing mode is initially present. For example, in a discharge where there are no pre-existing tearing modes or AEs, it could be possible to 'probe' the plasma by exciting and then immediately

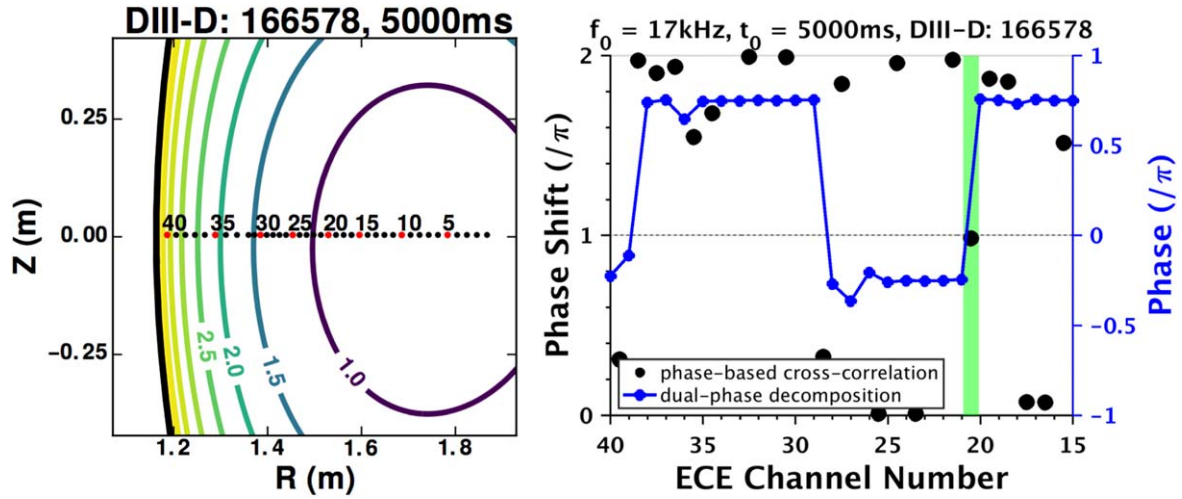

Figure 3. Left: positions of the ECE channels and q surfaces found with equilibrium reconstruction, placing the 17 kHz mode on the $q = 1$ surface. Right: mode localization from phase-based cross-correlation (points) and dual-phase decomposition (line) for the 16.5 kHz mode at 5001 ms in DIII-D discharge 166578. The mode is located between ECE channels 20 and 21.

stabilizing tearing modes with counter ECCD in order to generate a useful mode that is measurable with ECE. Should the acquired q-profile locations through ECE analysis not be sufficient, the possibility remains to supplement with q values extracted through other means, including established geometric formulas such as

$$q_{95} = q_{\mathrm{cyl}}\left(\frac{1.17 - 0.65\,a/R}{[1 - (a/R)^2\,]^2}\right), \tag{1}$$

where $q_{\mathrm{cyl}} = (\pi\ a^2\kappa B_T)/(\mu_0 I_p R)$ can be estimated as the engineering safety factor [39, 40]. Note that global magnetics measurements are necessary for this calculation. A mix of q values from multiple locations can help broaden the number of discharges to which this technique applies. These data can be used as calibration for other q-profile measurement techniques, including standard equilibrium reconstruction codes and MSE, or as a value-add to provide additional constraining data for q-profile and equilibrium determinations. Furthermore, it is useful to note that ECE-based q-surface location can benefit analysis when the precise location of just a single resonant mode is needed—for example the $q = 1/1$ mode during sawtooth studies.

Looking towards possible application on ITER, it is important to note that high electron temperatures ($T_e >$ 10 keV) will cause relativistic broadening of the ECE frequencies in addition to existing thermal broadening. This will result in spatial averaging of the ECE signals that is significantly larger than the ECE sampling width present in current magnetic fusion systems. Furthermore, at high electron temperatures ECE frequencies will also experience a relativistic shift towards the high-field side. These effects and their consequences for ECE diagnostics on ITER have been the subject of many studies [41–45]. For the purposes of q-profile localization it important to be able to resolve the locations of magnetic islands. The absorption spectrum $\alpha(s)$ and the resulting emissivity function $G(s)$ for three selected second harmonic ECE frequencies ($f_{ce} = 256$, 297 and 354 GHz) in an expected ITER H-mode plasma with

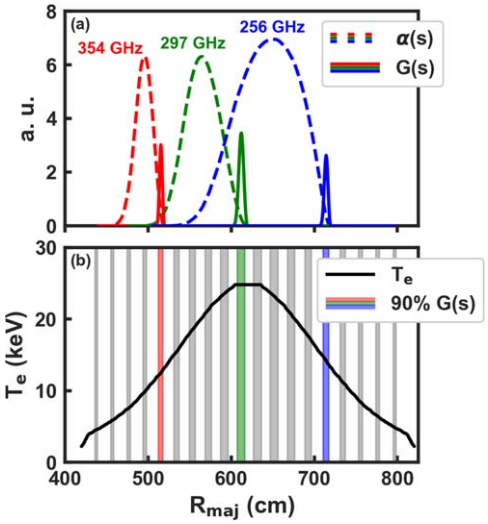

Figure 4. (a) The absorption coefficients $\alpha(s)$ and emissivity functions $G(s)$ are plotted as functions of major radius R_{maj} for three selected second harmonic ECE frequencies on ITER. (b) The temperature profile $T_e(R_{\mathrm{maj}})$ assumed for these calculations is an H-mode discharge with $T_{e,\max} = 25$ keV. The 90% width of each ECE frequency is over-plotted as vertical bars, showing measurement limitations due to broadening.

$T_{e,\max} = 25$ keV are shown in figure 4. In this paper the relativistic broadening for an ITER H-mode scenario was calculated using the ECESIM code [43], which has been benchmarked against the ECELS code used previously for ITER cases [46]. Both simulation codes follow the Bornatici formulation, including corrections for high T_e [41]. Spatial localization of the signal is determined by calculating the emissivity function

$$G(s) = T_{\mathrm{e}}(s)\alpha(s)\mathrm{e}^{-\tau(s)}, \tag{2}$$

where s is the spatial coordinate and τ is the optical depth [43]. The emission region is defined as the space along s resulting in 90% emission (between 5% and 95% of the

integral of $G(s)$). This emission width is shown for each frequency in figure 4(b), indicating that the radial resolution of each ECE channel should be high enough to localize individual locations along the q-profile. Note that these regions do not represent errors in ECE localization *per se*, but rather sampling region widths. Thus small islands can still be localized by interpolation. In-depth island localization studies [43, 44] motivated by NTM suppression have found that the required island width for ECE detection is on the order of $w = 2$ cm for the hottest case of $T_{e,\max} = 25$ kev. Further work has predicted that islands in the range of up to $w \sim 10$ cm can be tolerated in ITER before mode locking becomes inevitable and that ECE-NTM alignment within about 1 cm will be necessary for complete mode suppression [47, 48]. Under these considerations, islands in ITER should be both detectable and localizable, allowing for the construction of discrete points along the q-profile.

4. Production of an equilibrium from ECE

One of the most important analysis procedures related to tokamaks is the construction of a viable equilibrium. Unsurprisingly, ensuring the inclusion of a reliable q-profile is essential to this process [49]. Since integrated magnetics will be difficult to work with on ITER and DEMO, we apply the above methods of q-profile calculation to design a new, non-magnetic equilibrium reconstruction technique. In figure 2, the mode numbers were calculated with instantaneous magnetic data from Mirnov coils, which will be available on ITER. However, the use of Mirnov coils to determine $q = m/n$ could be avoided if the coverage of a radial ECE diagnostic is good enough to measure a mode on both sides of the plasma, or if an ECE-Imaging diagnostic was also employed [50]. For the purpose of this work it is further assumed that the magnetic boundary can be measured with imaging [19–21]. Two other functions are then required to solve the Grad–Shafranov equation, both of which can be obtained from ECE data. The three chosen input files are (1) the magnetic boundary in R, Z space: RZSEP(R, Z), (2) the safety factor across the plasma as a function of the normalized poloidal flux ψ_n: $q(\psi_n)$ and (3) the total pressure as a function of ψ_n: $P(\psi_n)$. While $P(\psi_n)$ cannot be directly realized from ECE, the symmetry mapping along flux contours ($R_{\text{out}}(R_{\text{in}}) \equiv$ locations of equal flux along a $Z = 0$ cross-section) can be extracted both from a measured $T_e(R)$ profile and from the equilibrium itself. This function can be used to iterate upon guesses for the required $q(\psi_n)$ and $P(\psi_n)$ profiles, as described below.

The proposed method is to use ECE measurements in addition to the Isolver code, which is a standalone free-boundary equilibrium solver that runs within TRANSP [51], to obtain an equilibrium. This is outlined schematically in figure 5. It is assumed that ECE coverage for a discharge is good enough to cover the entire radial extent of the plasma. This will allow for the measurement of $q(R)$ and $T_e(R)$ across the entire plasma. Along with the magnetic separatrix RZSEP (R, Z), initial guesses for $q(\psi_n)$ and $P(\psi_n)$ are used as inputs for the Grad–Shafranov solver, which uses Piccard iteration to satisfy the given constraints. In this work, the pressure profile guesses are defined by a fourth-order polynomial and the safety factor profiles are defined by a second-order polynomial in ι, where $q = 1/\iota$. For each pair of input guesses $q(\psi_n)$ and $P(\psi_n)$, the error of the resulting Grad–Shafranov solution is calculated by comparing the calculated $q(R)$ and PSIRZ(R, Z) to the discrete $q(R)$ and $T_e(R)$ profiles measured with ECE. The values of $q(R)$ are directly compared at mode locations where q can be experimentally measured. The symmetry $R_{\text{out}}(R_{\text{in}})$ of the calculated PSIRZ(R, Z) and measured $T_e(R)$ profiles are compared by mapping the inboard location of a flux/temperature to the outboard location of the same flux/temperature. Iterations are preformed to minimize the total error. Further development is necessary before this scheme can be generally applied, but it is shown here to yield reasonable results in a conceptual study.

For an arbitrary test equilibrium generated with Isolver for NSTX, the equilibrium reconstructed with this method is presented in figure 6. To test this calculation, a set of $q(\psi_n)$, $P(\psi_n)$ and RZSEP(R, Z) profiles were assumed as the background plasma. The ECE-based equilibrium, which was constructed entirely from four q locations measurable with ECE, a full $T_e(R)$ profile measurable with ECE and the separatrix boundary RZSEP(R, Z) measurable with plasma imaging, is presented in dashed red. It is compared to the results of full kinetic equilibrium reconstruction on the assumed $q(\psi_n)$, $P(\psi_n)$ and RZSEP(R, Z) profiles, which is presented in solid black. As seen in figure 6, the two methods are in good agreement. The error as a function of iteration is shown in figure 7, and is shown to relax exponentially with iteration number.

Since this reconstruction method utilizes existing Grad–Shafranov solvers based on Picard iteration, when developed it should be no slower than currently available equilibrium reconstruction schemes. Optimization of the solution could be executed simultaneously on a parallel gpu. A full quantization of the accuracy and speed of this technique would require several real shots with complete ECE coverage and is outside the scope of this paper. As such, developing a proof-of-concept with demonstrations on a wide variety of plasma scenarios will be the focus of future work. Additionally, it is predicted that it will not be possible to obtain a full T_e symmetry mapping during a discharge with $T_{e,\max} = 25$ keV due to reabsorption of signals from the high-field side. At these temperatures, only frequencies from the low-field side will leave the plasma, which is still enough information to construct a discrete q-profile. Construction of a full symmetry mapping profile will still be possible, however, during the ITER startup phase when plasma temperatures are lower and scenarios are not yet fully developed. Further distortion of the ECE signal may occur through asymmetric effects due to non-thermal electrons [52, 53]. Existing high-temperature tokamaks such as JET, TFTR, DIII-D, etc have shown differences between electron temperatures measured with ECE and TS, but the extent of this effect on ITER remains to be measured and is assumed to be manageable.

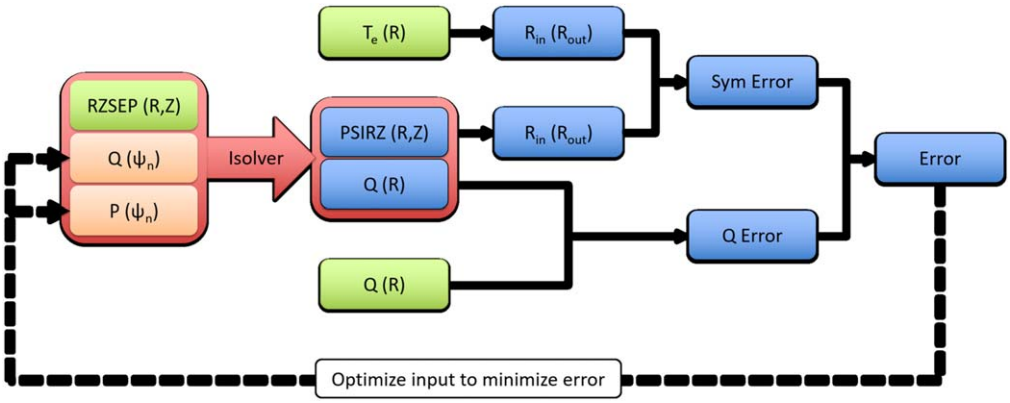

Figure 5. Schematic of the equilibrium-selection process using ECE and Isolver. Green boxes represent measured quantities, blue boxes represent calculated quantities, and orange boxes represent guessed profiles fed to Isolver. A 'best fit' equilibrium is chosen by minimizing the error between the the measured and calculated $q(R)$ profiles and the symmetry mappings $R_{out}(R_{in})$ of the calculated poloidal flux and the measured electron temperature.

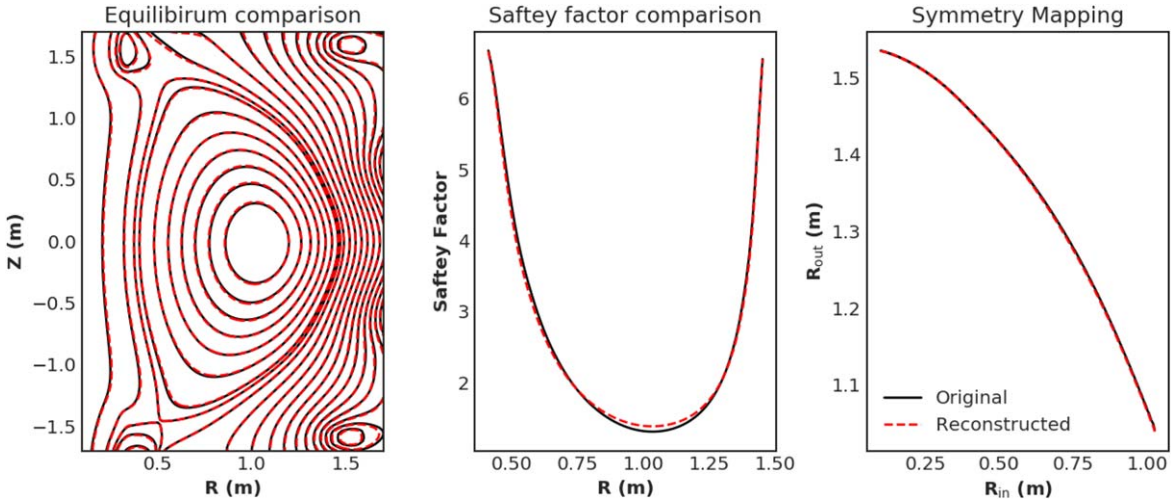

Figure 6. Comparison of equilibria generated with Isolver. The original equilibrium is plotted in black (solid) and was chosen as a random possible equilibrium for NSTX. The reconstructed equilibrium is plotted in red (dashed), and was produced by selecting a 'best fit' equilibrium using the methods described in the text.

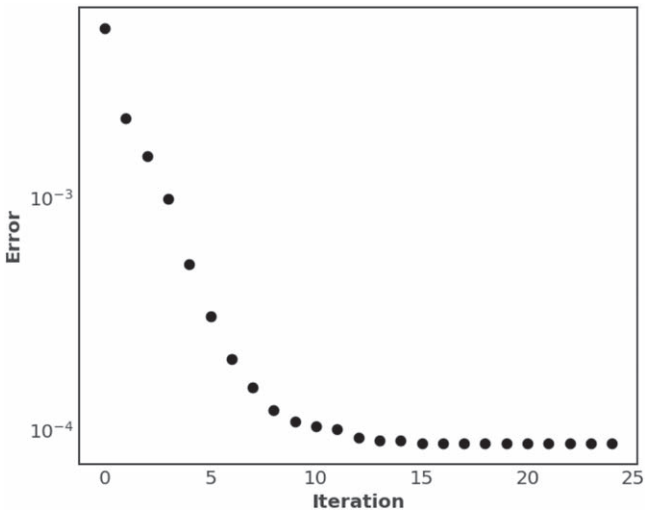

Figure 7. The error of the PSIRZ/T_e symmetry and $q(R)$ as a function of iteration number.

Finally, note that it is not necessary to fully develop this reconstruction scheme in order to apply the above techniques to existing tokamaks. ECE-measured q-profiles and symmetry conditions can be included as an additional constraint in existing magnetics-based equilibrium reconstruction processes. This would be a value-add for existing reconstruction codes and could potentially improve the robustness of kinetic equilibrium reconstruction in the high-neutron, long-pulse environments predicted in future machines.

5. Conclusion

Techniques previously developed to determine the radial location of tearing modes using ECE have been extended to discharges with multiple distinct magnetic modes. By measuring the radial location of each mode, a discrete q-profile can be constructed using a single multichannel ECE radiometer. Discrete q-profiles may be constructed with measurements from

- Alfvén eigenmodes for $q < 1$,
- Sawteeth for $q = 1$,
- Alfvén eigenmodes for $q_{\min}$,
- Tearing and mode activity for $q = m/n$, and
- Global magnetics for q_{95}.

A q-profile generated in this manner not only provides an independent check for profiles generated with other techniques, but can also be used for equilibrium reconstruction. To that end, we have presented the conceptual design of a non-magnetic equilibrium reconstruction algorithm that is based on imaging and ECE measurements, and have tested the scheme on a theoretical NSTX discharge. Estimates may be made of the plasma equilibrium by matching the output of a free-boundary equilibrium solver to the symmetries displayed by measured q and T_e profiles. This method does not rely on either integrated magnetic measurements, which can be difficult to use in long-pulse discharges, nor TS, which contains components that are highly sensitive to neutron damage. As such, a fully-developed ECE-based equilibrium reconstruction could provide a valuable constraint on equilibria calculated for ITER and beyond.

Acknowledgments

The authors would like to acknowledge Joshua Breslau (PPPL) for his assistance in running the Isovler code and Chris Holcomb (DIII-D) for his assistance generating E_R-corrected MSE constraints. This research was supported by the United States Department of Energy (DoE) under contract numbers DC-AC02-09Ch11466, DE-FC02-04ER54698 and DE-SC0015480.

Disclaimer

ORCID iDs

A O Nelson https://orcid.org/0000-0002-9612-1936

References

[1] Costley A E, Sugie T, Vayakis G and Walker C I 2005 Technological challenges of ITER diagnostics *Fusion Eng. Des.* **74** 109–19
[2] Litnovsky A, Voitsenya V S, Costley A and Donné A J H 2007 First mirrors for diagnostic systems of ITER *Nucl. Fusion* **47** 833–8
[3] Salewski M, Meo F, Bindslev H, Furtula V, Korsholm S B, Lauritzen B, Leipold F, Michelsen P K, Nielsen S K and Nonbøl E 2008 Investigation of first mirror heating for the collective Thomson scattering diagnostic in ITER *Rev. Sci. Instrum.* **79** 10E729
[4] Litnovsky A *et al* 2009 Progress in research and development of mirrors for ITER diagnostics *Nucl. Fusion* **49** 075014
[5] Leipold F *et al* 2016 Cleaning of first mirrors in ITER by means of radio frequency discharges *Rev. Sci. Instrum.* **87** 11D439
[6] Donné A J H *et al* 2007 Chapter 7: diagnostics *Nucl. Fusion* **47** S337–84
[7] Pandya H K B *et al* 2017 ITER ECE Diagnostic: design Progress of IN-DA and the diagnostic role for Physics *J. Phys.: Conf. Ser.* **823** 012033
[8] Taylor G *et al* 2017 Update on the status of the ITER ECE diagnostic design *EPJ Web Conf.* **147** 02003
[9] Park Y S and Welander A S 2006 Real-time determination of magnetic island location for neoclassical tearing mode control in DIII-D *Plasma Phys. Control. Fusion* **48** 1447
[10] Sharapov S E *et al* (JET-EFDA Contributors and EFDA-JET work programme) 2002 Alfvén wave cascades in a tokamak *Phys. Plasmas* **9** 2027–36
[11] Van Zeeland M A, Kramer G J, Austin M E, Boivin R L, Heidbrink W W, Makowski M A, McKee G R, Nazikian R, Solomon W M and Wang G 2006 Radial structure of alfvén eigenmodes in the DIII-D tokamak through electron-cyclotron-emission measurements *Phys. Rev. Lett.* **97** 135001
[12] Lao L L, St John H E, Peng Q, Ferron J R, Strait E J, Taylor T S, Meyer W H, Zhang C and You K I 2005 MHD equilibrium reconstruction in the DIII-D tokamak *Fusion Sci. Technol.* **48** 968–77
[13] Zhang C and Lao L L 2004 Plasma equilibrium reconstruction with new internal magnetic constraints *American Physical Society, 46th Annual Meeting of the Division of Plasma Physics* http://adsabs.harvard.edu/abs/2004APS..DPPJP1044Z
[14] Nowak S, Cirant S, Alessi E, Boncagni L, Crisanti F, Galperti C, Granucci G, Sozzi C and Vitale E 2011 Fast equilibrium reconstruction (FASTEQ) for the control in real time of MHD instabilities in FTU tokamak *38th EPS Conf. on Plasma Physics* p P4.085 http://ocs.ciemat.es/EPS2011ABS/pdf/P4.085.pdf
[15] Qian J P *et al* 2017 An efficient technique for magnetic equilibrium reconstruction with q profile constraints and its application on the EAST tokamak *Nucl. Fusion* **57** 084001
[16] Imazawa R, Kawano Y and Kusama Y 2011 A new approach of equilibrium reconstruction for ITER *Nucl. Fusion* **51** 113022
[17] Huang Y, Xiao B J J, Luo Z P P, Qian J P P, Li S, Chen Y, Liu H Q Q, Xu L Q Q, Yuan Y and Yuan Q P P 2017 Development of real-time plasma current profile reconstruction with POINT diagnostic for EAST plasma control *Fusion Eng. Des.* **120** 1–8
[18] Hommen G, de Baar M, Citrin J, De Blank H J, Voorhoeve R J, De Bock M F M M, Steinbuch M and JET-EFDA Contributors 2013 A fast, magnetics-free flux surface estimation and q-profile reconstruction algorithm for feedback control of plasma profiles *Plasma Phys. Control. Fusion* **55** 25007

[19] Hommen G, de Baar M, Nuij P, Mcardle G, Akers R and Steinbuch M 2010 Optical boundary reconstruction of Tokamak plasmas for feedback control of plasma position and shape *Rev. Sci. Instrum.* **81** 113504

[20] Hommen G, de Baar M, Duval B P, Andrebe Y, Le H B, Klop M A, Doelman N J, Witvoet G, Steinbuch M and the TCV Team 2014 Real-time optical plasma boundary reconstruction for plasma position control at the TCV Tokamak *Nucl. Fusion* **54** 073018

[21] Zhang H, Xiao B, Luo Z, Hang Q, Yang J and Weldon D 2018 Reconstruction of the plasma boundary of EAST tokamak using visible imaging diagnostics *IEEE Trans. Plasma Sci.* **46** 2162–9

[22] Berrino J, Lazzaro E, Cirant S, D'Antona G, Gandini F, Minardi E and Granucci G 2005 Electron cyclotron emission temperature fluctuations associated with magnetic islands and real-time identification and control system *Nucl. Fusion* **45** 1350–61

[23] Isayama A *et al* 2003 Achievement of high fusion triple product, steady-state sustainment and real-time NTM stabilization in high- p ELMy H-mode discharges in JT-60U *Nucl. Fusion* **43** 1272–8

[24] Keller A, Leuterer F, Maraschek M, Suttrop W, Zohm H and the ASDEX Upgrade Team 2003 Analysis methods and conditions for feedback controlled NTM stabilization *30th EPS Conf. on Contr. Fusion and Plasma Physics* vol 27A p P-1.130 https://pure.mpg.de/pubman/faces/ViewItemOverviewPage.jsp?itemId=item_2137563

[25] Nelson A O, La Haye R J, Austin M E, Welander A S and Kolemen E 2019 Simultaneous detection of neoclassical tearing mode and electron cyclotron current drive locations using electron cyclotron emission in DIII-D *Fusion Eng. Des.* **141** 25–9

[26] Kim K *et al* (the KSTAR Team) 2015 Experiment and simulation of tearing mode evolution with electron cyclotron current drive in KSTAR *Curr. Appl Phys.* **15** 547–54

[27] Bongers W A *et al* (the Textor Team) 2008 Magnetic island localization for NTM control by ECE viewed along the same optical path of the ECCD beam *Fusion Sci. Technol.* **55** 1536

[28] Volpe F A G *et al* 2009 Advanced techniques for neoclassical tearing mode control in DIII-D *Phys. Plasmas* **16** 102502

[29] Reich M, Bock A, Maraschek M and Asdex Upgrade Team, and the Asdex Upgrade Team 2012 NTM localization by correlation of Te and dB/dt *Fusion Sci. Technol.* **61** 309–13

[30] Strait E J 2006 Magnetic diagnostic system of the DIII-D tokamak *Rev. Sci. Instrum.* **77** 023502

[31] Austin M E and Lohr J 2003 Electron cyclotron emission radiometer upgrade on the DIII-D tokamak *Rev. Sci. Instrum.* **74** 1457

[32] Luce T C, Petty C C, Meyer W H, Holcomb C T, Burrell K H and Bergsten L J 2016 Method for correction of measured polarization angles from motional Stark effect spectroscopy for the effects of electric fields *Plasma Phys. Control. Fusion* **58** 125010

[33] Nave M F F *et al* (JET-EFDA Contributors) 2004 On the use of MHD mode analysis as a technique for determination of q-profiles in JET plasmas *Rev. Sci. Instrum.* **75** 4274–7

[34] Kramer G J, Oikawa T, Fujita T, Kamada Y, Kusama Y, Tobita K, Ozeki T, Cheng C Z and Nazikian R 1998 The determination of the q-profile in the plasma core from Alfvén eigenmodes *Plasma Phys. Control. Fusion* **40** 863–9

[35] Kramer G J, Cheng C Z, Kusama Y, Nazikian R, Takeji S and Tobita K 2001 Magnetic safety factor profile before and after sawtooth crashes investigated with toroidicity and ellipticity induced Alfvén eigenmodes *Nucl. Fusion* **41** 1135–51

[36] Lao L L *et al* 2009 Tearing-mode excitation by counter ECCD for validation of resistive MHD models in DIII-D *American Physical Society, 51st Annual Meeting of the APS Division of Plasma Physics* JP8.087 http://adsabs.harvard.edu/abs/2009APS..DPPJP8087L

[37] Hennen B A, Westerhof E, Nuij P W J M J M, Oosterbeek J W, de Baar M R, Bongers W A, Bürger A, Thoen D J, Steinbuch M and the TEXTOR Team 2010 Real-time control of tearing modes using a line-of-sight electron cyclotron emission diagnostic *Plasma Phys. Control. Fusion* **52** 104006

[38] Haye R J La *et al* 2016 Exploration of the means for real-time probing of $m/n = 2/1$ tearing mode stability evolution in the ITER baseline scenario in DIII-D *43rd EPS Conf. on Plasma Physics* http://ocs.ciemat.es/EPS2016PAP/pdf/P5.026.pdf

[39] Boucher D *et al* 1998 The International Multi-Tokamak Profile Database *Nucl. Fusion* **40** 302

[40] Stotler D P, Reiersen W T and Bateman G 1994 ASPECT: an advanced specified-profile evaluation code for tokamaks *Comput. Phys. Commun.* **81** 261–91

[41] Bornatici M, Cano R, De Barbieri O and Engelmann F 1983 Electron cyclotron emission and absorption in fusion plasmas *Nucl. Fusion* **23** 1153–257

[42] Bartlett D V 1996 Physics Issues of ECE and ECA for ITER *Diagnostics for Experimental Thermonuclear Fusion Reactors* ed P E Stott (Boston, MA: Springer) pp 183–92

[43] Austin M E 2011 Resolution of electron cyclotron emission measurements of magnetohydrodynamic modes in ITER *Fusion Sci. Technol.* **59** 647–50

[44] Van Den Brand H, De Baar M R, Lopes Cardozo N J and Westerhof E 2013 Evaluating neoclassical tearing mode detection with ECE for control on ITER *Nucl. Fusion* **53** 013005

[45] Austin M E, Brookman M W, Rowan W L, Danani S, Bryerton E W and Dougherty P 2016 Design and first plasma measurements of the ITER-ECE prototype radiometer *Rev. Sci. Instrum.* **87** 11E111

[46] Bartlett D V and Bindslev H 1998 Physics aspects of ECE Te measurements in ITER *Diagnostics for Experimental Thermonuclear Fusion Reactors 2* ed P E Stott *et al* (Boston, MA: Springer) pp 171–80

[47] La Haye R J, Prater R, Buttery R J, Hayashi N, Isayama A, Maraschek M E, Urso L and Zohm H 2006 Cross-machine benchmarking for ITER of neoclassical tearing mode stabilization by electron cyclotron current drive *Nucl. Fusion* **46** 451–61

[48] Van Den Brand H, De Baar M R, Lopes Cardozo N J and Westerhof E 2012 Integrated modelling of island growth, stabilization and mode locking: Consequences for NTM control on ITER *Plasma Phys. Control. Fusion* **54** 094003

[49] Taylor T S 1997 Physics of advanced tokamaks *Plasma Phys. Control. Fusion* **39** B47

[50] Tobias B, Grierson B A, Muscatello C M, Ren X, Domier C W, Luhmann N C, Zemedkun S E, Munsat T L and Classen I G J 2014 Phase-locking of magnetic islands diagnosed by ECE-imaging *Rev. Sci. Instrum.* **85** 11D847

[51] Andre R 2012 TRANSP/PTRANSP Isolver free boundary equilibrium solver *American Physical Society, 54th Annual DPP Meeting* http://adsabs.harvard.edu/abs/2012APS..DPPJP8123A

[52] Harvey R W, O'Brien M R, Rozhdestvensky V V, Luce T C, McCoy M G and Kerbel G D 1993 Electron cyclotron emission from nonthermal tokamak plasmas *Phys. Fluids* B **5** 446–56

[53] Subhash P V, Singh A K, Pandya H, Divya V S, Aparna M P and Basitha Thanseem T K 2017 A parametric model for contribution of superthermal electrons to oblique measurement electron cyclotron spectra under ITER-like conditions *Fusion Sci. Technol.* **72** 49–59